Extremum-seeking control for the adaptive design of variable gain controllers

Extremum-Seeking Control for the Adaptive Design of Variable Gain Controllers

Bram Hunnekens, Antonio Di Dino, Nathan van de Wouw, *Member, IEEE*, Niels van Dijk, and Henk Nijmeijer, *Fellow, IEEE*

***Abstract*— In this paper, we experimentally demonstrate an extremum-seeking control strategy for nonlinear systems with periodic steady-state outputs, for the adaptive design of variable-gain controllers. Variable-gain control can balance the tradeoff between low-frequency disturbance suppression and sensitivity to high-frequency noise in a more desirable manner than linear controllers can. However, the optimal performance-based tuning of the variable-gain controller parameters is far from trivial, and depends on the unknown disturbances acting on the system. The extremum-seeking controller only utilizes output measurements of the plant, and can therefore be used to optimally design the parameters of the variable gain controller, without using direct information on the disturbances acting on the system. Experimental results are presented for the performance-optimal tuning of a variable-gain controller applied to a magnetically levitated industrial motion control setup performing tracking motions. The influence of the different parameter choices on the performance of the extremum-seeking controller is illustrated through experiments.**

***Index Terms*— Extremum-seeking control, motion control, periodic steady-state performance, variable-gain control.**

I. Introduction

EXTREMUM seeking control is an adaptive control approach that optimizes a certain performance measure in terms of the steady-state output of a system in real time, by automated and continuous adaptation of the system parameters. In general, extremum-seeking control is typically used to optimize system performance in terms of constant steady-state outputs [2], [16], [24], [25]. Recently, an extremum-seeking control method has been proposed for steady-state performance optimization of general nonlinear plants with arbitrary periodic steady-state outputs of the plant [7]. Other works on the extremum-seeking control for systems with periodic steady-state outputs can be found in [6], [12], and [15]. We also note that besides the adaptive extremum-seeking approach we consider in this paper, which continuously adapts system parameters, extremum-seeking methods also exist, which iteratively update the system parameters in a periodic sampled-data fashion, in combination with a numerical optimization scheme [15], [27].

The application of extremum-seeking control for periodic steady-state outputs is generically relevant in the scope of periodic tracking problems and is particularly relevant in the context of motion control applications, such as industrial robotics, wafer scanners, and pick-and-place machines. In the latter application areas, periodic reference trajectories are often tracked to perform specific motion tasks. In this context, extremum-seeking control, in which neither a plant model nor disturbance models are required, is especially suitable for adaptive tuning controller parameters to obtain an optimal time-varying steady-state response, tuned for the (unknown) disturbances at hand.

In this paper, we will experimentally demonstrate the extremum-seeking control approach for periodic steady-states introduced in [7]. In particular, we will use the approach for the performance-optimal design of variable-gain controllers and will address an industrial motion control application. In industry, linear motion systems are still often controlled by linear controllers, mostly of the proportional–integral–differential type [1]. However, it is well known that linear controllers suffer from inherent performance limitations such as the waterbed effect [5]. This waterbed effect describes the well-known tradeoff between, on the one hand, low-frequency tracking and, on the other hand, sensitivity to high-frequency disturbances and measurement noise. If only low-frequency disturbances are present, a high-gain controller is preferred to obtain good low-frequency tracking properties. Contrarily, if only high-frequency disturbances and noise are present, a low-gain controller is preferred as not to amplify the effect of the high-frequency disturbances. Typically, a linear controller needs to balance between these two conflicting objectives with the waterbed effect as a constraint due to the Bode sensitivity integral.

To overcome such a performance limitation to a certain extent, a nonlinear variable-gain control strategy has been employed in [3], [10], [11], [28], [29], and [31]. In these references, it has been shown that variable-gain controllers have the capability of outperforming linear controllers in the scope of the tradeoff mentioned above, especially in

Manuscript received April 28, 2014; accepted July 12, 2014. Date of publication October 17, 2014; date of current version April 14, 2015. Manuscript received in final form September 24, 2014. This work was supported by the Dutch Technology Foundation. Recommended by Associate Editor M. Guay.

B. Hunnekens and H. Nijmeijer are with the Department of Mechanical Engineering, Eindhoven University of Technology, Eindhoven 5612 AZ, The Netherlands (e-mail: b.g.b.hunnekens@tue.nl; h.nijmeijer@tue.nl).

A. Di Dino was with the University of Trento, Trento 38122, Italy and is currently with the Department of Research and Development, PAMA s.p.a., Rovereto, Italy (e-mail: antonio.didino@unitn.it).

N. van de Wouw is with the Department of Mechanical Engineering, Eindhoven University of Technology, Eindhoven 5612 AZ, The Netherlands, and also with the University of Minnesota, Minneapolis, MN 55455 USA (e-mail: n.v.d.wouw@tue.nl).

N. van Dijk is with Philips Innovation Services, Eindhoven 5656 AE, The Netherlands (e-mail: niels.van.dijk@philips.com).

Color versions of one or more of the figures in this paper are available online at http://ieeexplore.ieee.org.

Digital Object Identifier 10.1109/TCST.2014.2360913

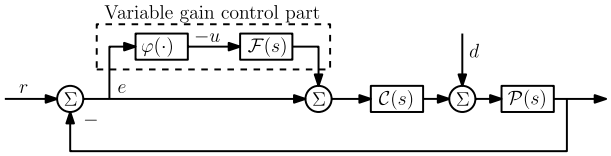

Fig. 1. Closed-loop variable-gain control scheme.

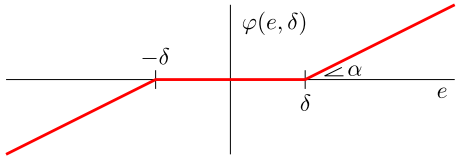

Fig. 2. Nonlinearity $\varphi(e,\delta)$ discriminating between small errors and large errors.

the scope of nonstationary or nonlinear disturbance and/or performance specifications. Although these controller designs are intuitive in nature, an optimal performance-based tuning of such variable-gain controllers is far from trivial, especially as it depends on the particular disturbance situation at hand. As a consequence, suboptimal tuning is typically done in a heuristic fashion.

In this paper, we therefore propose to employ extremum-seeking to optimally tune the variable-gain controller parameters, without using knowledge on the disturbances acting on the system. The benefits of the adaptive tuning of variable-gain controller parameters have been shown in an iterative feedback tuning context in [8] and [9]. Here, we will not employ such an iterative approach, but we will use an alternative adaptive approach based on the extremum-seeking technique for periodic steady-states, which does not use any plant model, unlike the approach in [8] and [9], and does not use explicit knowledge on the disturbances, as in [19].

The main contributions of the paper can be summarized as follows.

1) First, we present the experimental validation of the extremum-seeking strategy for periodic steady-states presented in [7] in the context of optimizing variable-gain controllers for repetitive motion tasks.
2) Second, we show that the tracking performance of industrial motion control systems can be significantly improved (compared to linear controllers) using variable gain controllers optimally tuned by extremum-seeking.

This paper extends the preliminary results in [13], in particular by experimentally validating the extremum-seeking approach for periodic steady states, by application to an industrial motion control setup, and by giving more specific tuning guidelines for the extremum-seeking controller.

The remainder of the paper is organized as follows. In Section II, we discuss the problem formulation considered in this paper. In Section III, we discuss the extremum-seeking control strategy for systems with periodic steady-states in the scope of the adaptive optimization of variable-gain controllers. The industrial motion control setup and nominal variable-gain controller design for this system will be discussed in Section IV. In Section V, the experimental results of the extremum-seeking control strategy for the performance-optimal tuning of the variable-gain controller will be presented. The conclusion will be presented in Section VI.

II. Problem Formulation

Consider the closed-loop variable-gain control scheme shown in Fig. 1, with the underlying linear control structure consisting of the linear plant dynamics and the nominal linear controller with transfer functions $\mathcal{P}(s)$ and $\mathcal{C}(s)$, $s \in \mathbb{C}$, respectively, reference signal r, force disturbance d, and tracking error signal e. To enhance the performance of the closed-loop system with respect to that achievable by the linear controller $\mathcal{C}(s)$, we introduce a nonlinear element $\varphi(e,\delta)$ and shaping filter $\mathcal{F}(s)$. The design of $\mathcal{F}(s)$ will relate to shaping the positive-real properties of the closed-loop system, as we will illustrate in Section V. The choice of the shape of the nonlinearity $\varphi(e,\delta)$ is given by a dead-zone characteristic

$$\varphi(e,\delta) = \begin{cases} \alpha(e+\delta), & \text{if } e < -\delta \\ 0, & \text{if } |e| \le \delta \\ \alpha(e-\delta), & \text{if } e > \delta \end{cases} \tag{1}$$

with dead-zone length $\delta \ge 0$ and additional gain $\alpha \ge 0$ (Fig. 2). The particular tuning of the nonlinearity φ is key to optimizing performance, as we will show later. Let us now explicate the rationale behind the choice for the dead-zone characteristic. Typically, in motion systems, errors induced by low-frequency disturbances are larger in amplitude than those induced by high-frequency disturbances [29]. Therefore, if the error signal $e(t)$ exceeds the dead-zone level δ, an additional controller gain α is induced, yielding superior low-frequency tracking and disturbance suppression properties. If, however, the error signal does not exceed the dead-zone length δ, no additional gain is induced as to avoid the deterioration of the sensitivity to high-frequency disturbances.

Remark 1: In addition to the particular dead-zone characteristic in (1), also other choices for the shape of the nonlinearity $\varphi(e,\delta)$ are possible, and can as well give performance benefits. However, for the sake of clarity of presentation of the variable-gain control strategy, and because we will use the dead-zone nonlinearity for the experimental setup in Section V, we will limit the analysis here to the specific dead-zone characteristic in (1).

Due to the choice of the variable-gain control structure in Fig. 1, the closed-loop dynamics can be modeled as a Lur'e-type system [14] of the form

$$\dot{x} = Ax + Bu + B_w w(t) \tag{2a}$$
$$e = Cx + D_w w(t) \tag{2b}$$
$$u = -\varphi(e,\delta) \tag{2c}$$

with state $x \in \mathbb{R}^n$, where $w(t) \in \mathbb{R}^m$ contains all external inputs, such as the reference $r(t)$ and force disturbance $d(t)$. The transfer function $\mathcal{G}_{eu}(s)$ denotes the transfer from input $u \in \mathbb{R}$ to output $e \in \mathbb{R}$ (Fig. 1), and can be expressed as

$$\mathcal{G}_{eu}(s) = C(sI - A)^{-1}B = \frac{\mathcal{P}(s)\mathcal{C}(s)\mathcal{F}(s)}{1 + \mathcal{P}(s)\mathcal{C}(s)}. \tag{3}$$

In motion control applications, performance relates to the size of the tracking error e. A key performance parameter

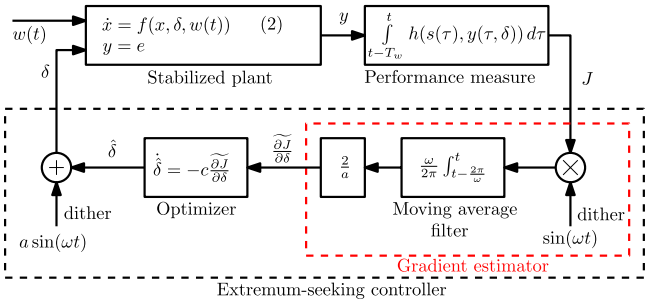

Fig. 3. Extremum-seeking scheme for the optimal tuning of the dead-zone length δ.

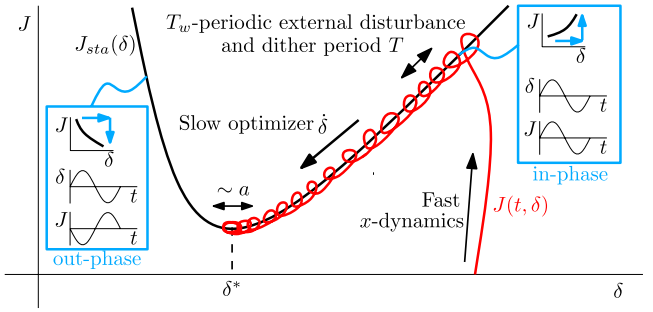

Fig. 4. Schematic representation of extremum-seeking procedure: the essential time-scales are also indicated.

in the variable gain control scheme in Fig. 1 is the dead-zone length δ, which discriminates between small and large errors (Fig. 2). The optimal value for δ that minimizes tracking errors, depends strongly on the external disturbances acting on the system. Because accurate disturbance models are difficult to obtain, and because the disturbances signature may change over time, a (fixed) heuristic choice of the dead-zone length δ as in [10] and [11] will likely be suboptimal. This makes the search for the performance-optimal δ a challenging task. The problem we consider in this paper is therefore *the online and adaptive performance-optimal tuning of the dead-zone length δ, without using knowledge on the disturbance situation at hand*.

We will approach this problem using the extremum-seeking control strategy for nonlinear systems with periodic steady-state outputs. This extremum-seeking strategy will be discussed in Section III. Subsequently, the approach will be applied to a variable-gain controlled experimental motion stage in Sections IV and V.

III. Extremum-Seeking for Periodic Steady-States

Extremum-seeking control is commonly used to optimize the performance of plants with constant steady-state outputs (i.e., in an equilibrium setting) [2], [16], [24], [25]. Compared with this extremum-seeking work for constant steady-states, extremum-seeking control for plants with time-varying outputs has received relatively little attention [6], [7], [12]. We will employ an extremum-seeking scheme for the performance optimization of nonlinear plants with *periodic* steady-state outputs, which is particularly relevant in the scope of tracking and disturbance rejection problems for motion systems, as we will show in Section V.

Consider the extremum-seeking scheme shown in Fig. 3, which, in the spirit of [18], consists of a stabilized plant (2), a performance output that is the tracking error $y = e$, a performance measure J that depends on the performance output $y = e$ (for example, typically of the integral squared error form $J = \int y^2 = \int e^2$), a gradient estimator, and an optimizer. In addition, the stabilized plant in the extremum-seeking scheme in Fig. 3 is subject to a bounded T_w-periodic input $w(t)$, which will give rise to time-varying outputs y of the stabilized plant.

Let us elaborate on the different elements in this extremum-seeking scheme in the scope of the variable-gain motion control setting specified in the previous section; for more details, we refer to [7].

1) Stabilized Plant: The stabilized plant can be a nonlinear system, which in this paper is the closed-loop variable-gain control system (2)

$$f(x, \delta, w) = Ax - B\varphi(e, \delta) + B_w w \tag{4}$$

in Fig. 3. Note that the extremum-seeking controller only uses output measurements of the stabilized plant, which can therefore be unknown. In the motion control context, the important performance output variable y is the tracking error, i.e., $y = e$.

2) Performance Measure: We aim to find the value of the dead-zone length δ that optimizes a performance measure J that depends on the T_w-periodic[1] steady-state performance output $\bar{y}_w(t, \delta)$ of the stabilized plant (2) [where we write $\bar{y}_w$ to emphasize that we consider the *steady-state* output that depends on the external T_w-periodic input $w(t)$]. To do so, the performance of the variable-gain controller is characterized by the performance measure

$$J(t, \delta) = \int_{t-T_w}^{t} h(s(\tau), y(\tau, \delta))d\tau. \tag{5}$$

Herein, h is a performance-related function to be chosen by the user and the T_w-periodic function $s(t)$ is a selection function allowing to weigh the error only in an important performance window (see Section IV for more details). Note that the output of the performance measure J as in (5) is constant if $y(t, \delta)$ is T_w-periodic in t for fixed δ.

As an example of a typical performance measure for a motion control application, consider the integral squared error performance measure

$$J(t, \delta) = \int_{t-T_w}^{t} e^2(\tau, \delta)d\tau \tag{6}$$

which relates to the tracking error e (Fig. 1) during the last T_w s.

3) Gradient Estimator: The gradient estimator uses dither, Figs. 3 and 4, to obtain an estimate $\widetilde{\partial J}/\partial\delta$ of the true gradient $\partial J_{\text{sta}}/\partial\delta$ of the unknown static performance map

$$J_{\text{sta}}(\delta) = \int_{0}^{T_w} h(s(\tau), \bar{y}_w(\tau, \delta))d\tau \tag{7}$$

[1]Later we will show under which conditions the steady-state output to T_w-periodic disturbances $w(t)$ is indeed T_w-periodic.

i.e., the performance map (5) for fixed δ and steady-state error $\bar{y}_w(t,\delta) = \bar{e}_w(t,\delta)$ (Fig. 4). The moving average filter in the gradient estimator (Fig. 3) is beneficial to filter out the oscillations with dither frequency ω in the performance J, thereby resulting in an improved gradient estimate $\widetilde{\partial J/\partial\delta}$ [7, Remark 7]. Note that the moving average filter serves a similar purpose as the low-pass and/or high-pass filters as applied in [25].

Optimizer: The extremum-seeking controller aims to find the minimum of the unknown steady-state performance map $J_{\text{sta}}(\delta)$, which we assume to be attained at δ^* (Fig. 4). The estimated gradient $\widetilde{\partial J/\partial\delta}$ is used by the optimizer

$$\dot{\hat{\delta}} = -c\widetilde{\frac{\partial J}{\partial \delta}} \tag{8}$$

to steer the nominal value $\hat{\delta}$ of the dead-zone length δ toward the performance optimizing value δ^*, with adaptation gain c, where

$$\delta = \hat{\delta} + a\sin(\omega t) \tag{9}$$

with a the dither amplitude, and $\omega = 2\pi/T$ the dither frequency (with dither period T).

A. Time Scale Separation

As in all classical extremum-seeking approaches [16], [24], [25], the principle of time-scale separation is essential to the successful operation of the extremum-seeking loop (Fig. 4). If the dither amplitude a, the dither frequency ω, and the adaptation gain c are chosen small enough to enable time-scale separation of the plant, gradient estimator, and optimizer, the performance $J(\delta)$ will remain close to the steady-state performance map $J_{\text{sta}}(\delta)$ (Fig. 4). In that case, the dither signal $\sin(\omega(t))$ will be in-phase (out-phase) with the measured performance $J(t,\delta)$ in case δ lies to the right (to the left) of the optimum θ^* (Fig. 4). This forms the basis for the gradient estimate $\widetilde{\partial J/\partial\delta}$ since the product of $\sin(\omega t)$ and $J(t,\delta)$ (Fig. 4) will be proportional to the true gradient $\partial J_{\text{sta}}/\partial\delta$. Hence, for sufficiently small c, a, and ω, it holds that $\widetilde{\partial J/\partial\delta}$ will be a good estimate of the true gradient $\partial J_{\text{sta}}/\partial\delta$ [24, Sec. 3.3] or [7, Remark 7] for the mathematical details.

The fact that we are optimizing performance in terms of T_w-periodic outputs (rather than equilibrium points) introduces an additional time scale. This time scale relates to the time period T_w of the periodic disturbances $w(t)$ and, although present in [7], this time scale was not explicitly discussed in that work. In the absence of such external inputs, i.e., in the extremum-seeking setting for *constant* steady-state outputs (the equilibrium setting) [2], [16], [24], [25], it is important that the dither frequency ω is chosen sufficiently low (T sufficiently high) compared with the time-scale of the plant dynamics. This guarantees that the plant operates close to its steady-state behavior, and hence, the performance J is close to its steady-state performance $J_{\text{sta}}(\delta)$ (Fig. 4) [25]. In the extremum-seeking setting for periodic steady-states as considered here, the performance $J(t,\delta)$ in (5) relates to the output response over the last T_w s. Additional to the requirement in the equilibrium case, it is therefore important that the dither period T is chosen sufficiently high compared with the period T_w of the inputs. This guarantees that δ is perceived as constant over one period T_w, such that the performance $J(t,\delta)$ is close to the steady-state performance $J_{\text{sta}}(\delta)$. On summarizing, the following essential time-scales are present in the extremum-seeking approach for periodic steady-states from fastest to slowest: 1) plant-dynamics; 2) period T_w of external disturbance; 3) dither period T; and 4) time scale of the optimizer related to the adaptation gain c.

Remark 2: Note that the inclusion of the selection function $s(t)$ in the definition of the performance measure (5) was not included in [7]. However, since the selection function $s(t)$ is also periodic with period time T_w, the function $h(s(t), y(t,\delta))$ in (5) is also periodic with period time T_w and is, moreover, bounded for bounded x and $w(t)$. Therefore, the output of the performance measure $J(t,\delta)$ will still be constant if the steady-state output $\bar{y}_w(t) = \bar{e}_w(t)$ is T_w periodic such that the results in [7] can be employed.

B. Stability Conditions

The following essential assumptions are made in [7, Th. 8] to guarantee the stability of the extremum-seeking scheme presented above.

- *A1:* The external inputs $w(t)$ are generated by an exosystem $\dot{w} = g(w)$ that generates uniformly bounded, T_w-periodic disturbances with a known constant period T_w.
- *A2:* For all *fixed* parameters $\delta \in \mathbb{R}$, the nonlinear system (2) exhibits a unique globally asymptotically stable steady-state solution $\bar{x}_w(t,\delta)$, with the same period time T_w.
- *A3:* The sufficiently smooth steady-state performance map $J_{\text{sta}}(\delta)$ has a unique global minimum at δ^*.
- *A4:* The vector field $f(x,\delta,w)$ of the stabilized plant in (4) is twice continuously differentiable in x and δ, and continuously in $w(t)$.

Under these assumptions, the stability result in [7] guarantees that the closed-loop system is semiglobally practically asymptotically stable (SGPAS) in the following sense. For any $\rho_{x,i}, \nu_{x,i} \in \mathbb{R} > 0$, $i \in \{1,\ldots,n\}$, ρ_δ, $\nu_\delta \in \mathbb{R} > 0$ and initial conditions satisfying $\max_{s\in[-T_w,0]}|\tilde{x}_i(s)| \le \rho_{x,i}$ $\forall i \in \{1,\ldots,n\}$, $\max_{s\in[-T_w,0]}|\tilde{\delta}(s)| \le \rho_\delta$, there exist sufficiently small values for the dither amplitude a, dither frequency $\omega(a)$, and adaptation gain $c(a,\omega)$, such that the solutions $x(t)$ and $\delta(t)$ of the closed-loop extremum-seeking scheme are well defined for all $t \ge 0$ and satisfy the following properties:

1) uniform boundedness: $\sup_{t\ge0}|\tilde{x}_i(t)| \le C_{x,i}$ $\forall i \in \{1,\ldots,n\}$ and $\sup_{t\ge0}|\tilde{\delta}(t)| \le C_\delta$;
2) ultimate boundedness: $\limsup_{t\to\infty}|\tilde{x}_i(t)| \le \nu_{x,i}$ $\forall i \in \{1,\ldots,n\}$ and $\limsup_{t\to\infty}|\tilde{\delta}(t)| \le \nu_\delta$

for some constants $C_{x,i}(\rho_{x,i},\rho_\delta,a,c,\omega), C_\delta(\rho_{x,i},\rho_\delta,a,c,\omega) \in \mathbb{R} > 0$, $i \in \{1,\ldots,n\}$, and where $\tilde{x}(t) := x(t) - \bar{x}_w(t,\delta)$ and $\tilde{\delta}(t) = \hat{\delta}(t) - \delta^*$. Note that the above codependence of the parameters a, ω, and c, indicate an order of tuning for the extremum-seeking parameters.

Remark 3: Under the assumptions stated above, [7, Th. 8] guarantees that the extremum-seeking scheme is SGPAS

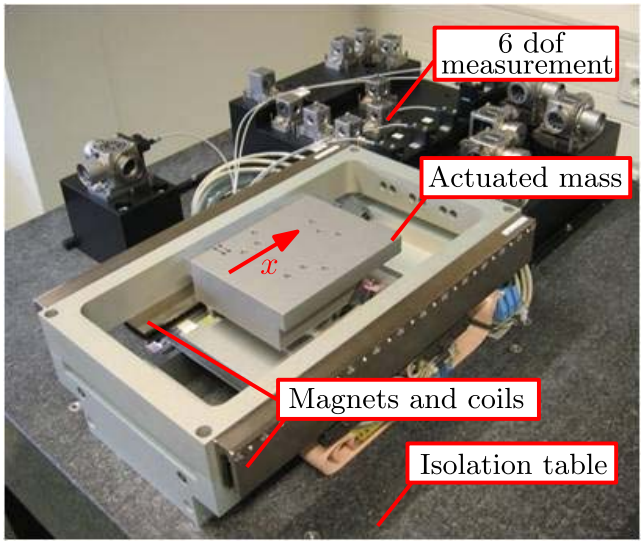

Fig. 5. Experimental setup: a magnetically levitated industrial motion platform with 6 degrees of freedom.

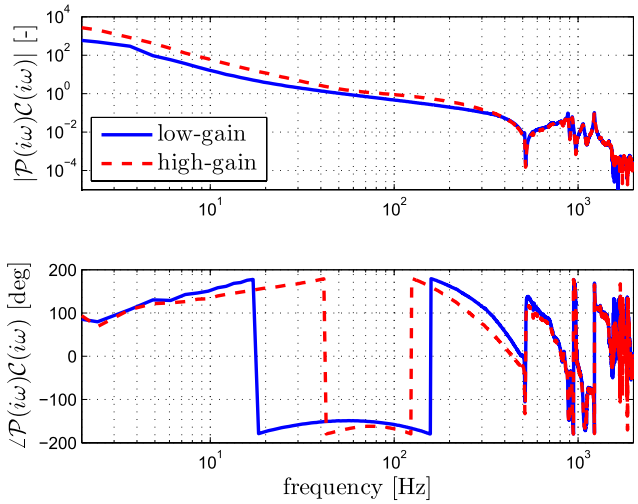

Fig. 6. Measured open-loop frequency response function $\mathcal{P}(i\omega)\mathcal{C}(i\omega)$ for the linear low-gain controller $\mathcal{C}(s)$ ($\delta = \infty$) and linear high-gain controller $\mathcal{C}(s)(1 + \alpha\mathcal{F}(s))$ ($\delta = 0$).

according to [7, Def. 1], which differs slightly from definitions of SGPAS in [25], which also considers the decay rate of the solutions.

IV. Experimental Setup and Nominal Controller Design

In this section, we will discuss the experimental setup that we will use to illustrate the practical feasibility of the control strategy proposed in the previous section. The magnetically levitated industrial motion platform itself will be discussed in Section IV-A. The nominal variable gain controller design will be discussed in Section IV-B, after which we will discuss the set-point and disturbance characterization in Section IV-C, and the performance specification in Section IV-D.

A. Magnetically Levitated Motion Platform

The plant $\mathcal{P}(s)$ is represented by the experimental setup in Fig. 5. The motion platform involves a magnetically levitated and magnetically actuated inertia, which can be controlled in all of its six degrees of freedom. Such a motion platform is suitable for application in, for example, pick-and-place machines or wafer scanners. The permanent magnets are attached to the fixed world, and the coils are attached to the actuated inertia. The main degree of freedom, the one that has the longest possible stroke (80 mm), is the x-direction (Fig. 5), which is also the direction that we will focus on. The remaining degrees of freedom are stabilized; this enables to position the actuated inertia accurately in all six degrees of freedom (which would not be possible using a fixed guide rail for example). All six degrees of freedom can be measured with an interferometer system which has a resolution of 0.625 nm. The whole setup, including the measurement system, is placed on a vibration isolation table.

B. Nominal Variable-Gain Controller Design

From frequency response measurements at different x-positions, it is observed that the plant can very well be considered linear. A stabilizing nominal (low-gain) linear controller $\mathcal{C}(s)$ (Fig. 1) has been designed using loop-shaping arguments [23], based on these frequency response measurements. It is stressed once more that the frequency response data of the plant $\mathcal{P}(i\omega)$ is only used to design this stabilizing controller $\mathcal{C}(s)$ and to verify the conditions of Theorem 1, and that no model of the plant is used explicitly by the extremum-seeking controller. The nominal linear controller consists of a lead-filter, a notch-filter, an integral action, and a second-order low-pass filter. The resulting measured open-loop frequency response function $\mathcal{P}(i\omega)\mathcal{C}(i\omega)$ is shown in Fig. 6. The open-loop bandwidth of the system is 52 Hz for the low-gain controller.

A linear controller with a higher loop-gain, and hence a higher bandwidth (of 86 Hz), has also been designed to achieve a higher level of low-frequency disturbance suppression. However, due to the waterbed effect [22], this low-frequency (below the bandwidth) performance improvement will lead to a deterioration of high-frequency (above the bandwidth) disturbance sensitivity. To balance this tradeoff in a more desirable manner, we therefore design a variable gain controller (Section II).

The following theorem provides sufficient conditions under which system (2), excited by a T_w-periodic input $w(t)$, has a uniquely defined T_w-periodic globally exponentially stable steady-state solution.

Theorem 1 [29], [30]: Consider system (2). Suppose:

B1: the matrix A is Hurwitz;

B2: the continuous nonlinearity $\varphi(e, \delta)$ satisfies

$$0 \leq \frac{\varphi(e_2, \delta) - \varphi(e_1, \delta)}{e_2 - e_1} \leq \alpha \tag{10}$$

for all $e_1, e_2 \in \mathbb{R}$, $e_1 \neq e_2$ and all $\delta \geq 0$;

B3: the transfer function $\mathcal{G}_{eu}(s)$ given by (3) satisfies

$$Re\left(\mathcal{G}_{eu}(i\omega)\right) > -\frac{1}{\alpha} \quad \forall \omega \in \mathbb{R}. \tag{11}$$

Then for any bounded T_w-periodic piecewise continuous input $w(t)$, system (2) has a unique T_w-periodic solution $\bar{x}_w(t)$,

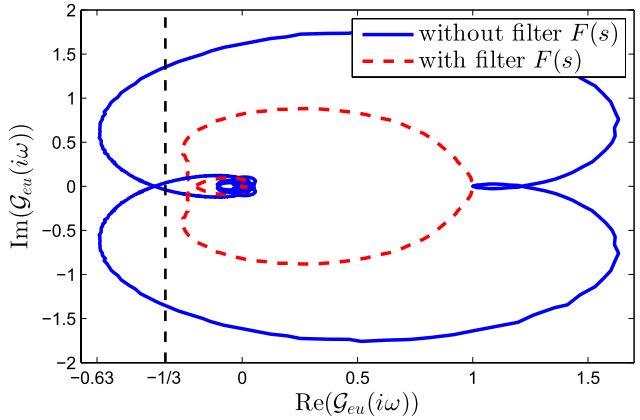

Fig. 7. Frequency-domain condition (11) illustrating that $\mathrm{Re}(\mathcal{G}(i\omega)) > -1/\alpha$ $\forall\omega \in \mathbb{R}$, on the basis of measured frequency response data.

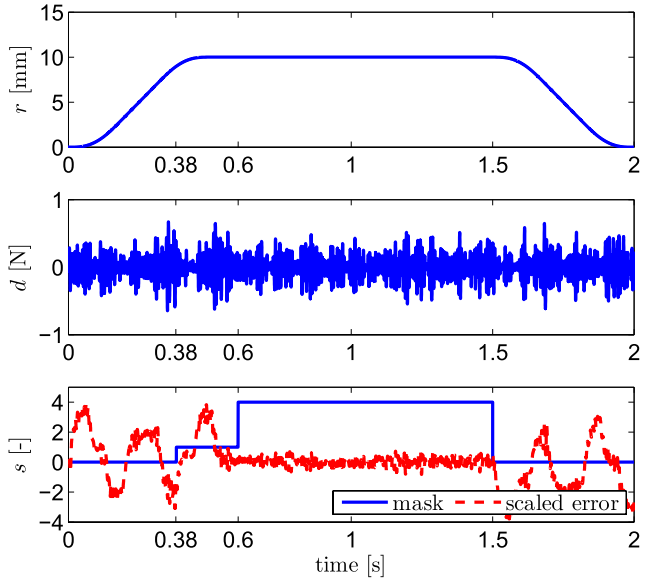

Fig. 8. Illustration of the T_w-periodic reference input $r(t)$, force-disturbance $d(t)$, and mask function $s(t)$ in (14).

which is globally exponentially stable and bounded for all $t \in \mathbb{R}$.

Systems with such a uniquely defined globally exponentially stable steady-state solution [for arbitrary bounded inputs $w(t)$] are called exponentially convergent [4], [20]. Note that the satisfaction of the conditions of Theorem 1 implies that Assumption A2 is satisfied. Indeed, the stabilized plant will then have a unique, T_w-periodic globally exponentially stable steady-state solution $\bar{x}_w(t, \delta)$ for fixed δ and T_w-periodic inputs $w(t)$. Note that this property guarantees the existence and uniqueness of the steady-state performance map $J_{\mathrm{sta}}(\delta)$ [21], which relates to Assumption A3. Of course, the existence of a unique global minimum δ^* depends on the specific problem (and performance specifications) considered.

Tuning of the shaping filter $\mathcal{F}(s)$ (Fig. 1) aims at adding a significant amount of allowable additional gain α, while satisfying the frequency-domain circle-criterion stability condition (11). Consider Fig. 7, where $\mathcal{G}_{eu}(i\omega)$ (3) is shown for the case without shaping filter $\mathcal{F}(s)$ (i.e., $\mathcal{F}(s) = 1$). If no shaping filter $\mathcal{F}(s)$ is used, the maximum additional gain is $\alpha = -1/-0.63 = 1.6$ (Fig. 7). Using a notch filter and low-pass filter, we constitute the shaping filter as follows:

$$\mathcal{F}(s) = \frac{\omega_p^2}{\omega_z^2}\frac{s^2 + 2\beta_z\omega_z s + \omega_z^2}{s^2 + 2\beta_p\omega_p s + \omega_p^2}\frac{\omega_{lp}^2}{s^2 + 2\beta_{lp}\omega_{lp} s + \omega_{lp}^2} \tag{12}$$

where $\omega_p = 40 \cdot 2\pi$ rad/s, $\omega_z = 60 \cdot 2\pi$ rad/s, $\beta_p = 1$, and $\beta_z = 0.5$, $\omega_{lp} = 2\pi 300$, and $\beta_{lp} = 0.7$, a higher additional gain $\alpha = -1/-0.26 = 3.8$ is allowed. We choose $\alpha = 3$ to have some guaranteed robustness, as indicated by the dashed vertical line in the circle criterion plot in Fig. 7. The loop-gain $\mathcal{P}(s)\mathcal{C}(s)$ is depicted for the linear controller limits of the variable-gain controllers, i.e., the linear low-gain ($\delta = \infty$) controller $\mathcal{C}(s)$ and high-gain ($\delta = 0$) controller $\mathcal{C}(s)(1 + \alpha\mathcal{F}(s))$, are depicted (by means of the open-loop frequency response functions) in Fig. 6.

By design of the stabilizing controller $\mathcal{C}(s)$, condition B1 of Theorem 1 is satisfied. Because we consider nonlinearities of the dead-zone type (1), condition B2 of Theorem 1 is also satisfied. Moreover, from Fig. 7, we conclude that condition B3 of Theorem 1 is also satisfied. Hence, system (2) has a unique, bounded, T_w-periodic, globally exponentially stable steady-state solution $\bar{x}_w(t)$ for T_w-periodic inputs. From this fact, we conclude that Assumption A2 needed for the extremum-seeking strategy is also satisfied.

Note that from Theorem 1, it follows that the dead-zone length δ of the nonlinearity is completely stability-invariant. This freedom is used in Section V to tune δ in a performance-optimal way using the extremum-seeking strategy from Section III.

C. Input Specification

To represent a realistic industrial application, the experimental setup considered will be tested in a tracking experiment where typical high-frequency disturbances are present. The reference $r(t)$ to be tracked by the magnetically levitated inertia [in the x-direction (Fig. 5)] consists of a third-order motion profile (Fig. 8). As a possible application, we consider a typical pick-and-place operation. Namely, on the reference, the inertia is moved from a zero-position to a 1 cm position (Fig. 8). Here, a component could be placed, for example, after which the movement is made back to the zero-position, resulting in a $T_w = 2$ second trajectory. In a typical industrial motion setting, also high-frequency (above the bandwidth) force disturbances will also be present (such as acoustic disturbances, or cross-talk from other parts of the machine, or measurement noise). To emulate such disturbances, we inject a high-frequency (colored, above the bandwidth) force disturbance to $d(t)$ (Fig. 8). Since the colored disturbance $d(t)$ has its main frequency content above 100 Hz (above the bandwidth), this is well separated from the frequency of 0.5 Hz of the reference signal $r(t)$ such that $d(t)$ can easily be approximated as being periodic with period time $T_w = 2$ s (Fig. 8). In addition, the configuration of the magnets and coils in the setup give rise to position-dependent cogging disturbances, which can also be considered to be approximately

periodic due to the periodic motion profile (and small tracking errors, such that $y \approx r$). The T_w-periodic reference $r(t)$ and force disturbance $d(t)$, with resulting (bounded) T_w-periodic external input $w(t) = [r(t), d(t)]^T$, could in principle be generated by an exo-system as stated in Assumption A1. From this, we conclude that Assumption A1 needed for the extremum-seeking strategy is satisfied.

D. Performance Specification

The inputs r and d as considered in Fig. 8 result in a measured closed-loop error response, as shown in the lower-plot in Fig. 8, for the nominal low-gain controller $\mathcal{C}(s)$. The performance objective relates to the important time at which the set point reaches the constant position phase (as an example, in a pick and place operation, high accuracy is needed here to place a component on a printed circuit board) (Fig. 8). Our goal will be to improve the low-frequency response (due to the acceleration phases, with unavoidable non-perfect feed-forward compensation) while not deteriorating the high-frequency error response during the constant position part (Fig. 8). To quantify both these effects in one performance measure, we define, in accordance with (5)

$$J(t,\delta) = \int_{t-T_w}^{t} s(\tau) e^2(\tau,\delta) d\tau \tag{13}$$

with the mask-function

$$s(t) = \begin{cases} 1, & \text{if } t \in [0.38, 0.6] + kT_w \\ 4, & \text{if } t \in [0.6, 1.5] + kT_w \\ 0, & \text{otherwise} \end{cases} \tag{14}$$

with $k \in \{0, 1, ...\}$, and $T_w = 2$ s (Fig. 8). A weight of $s(t) = 4$ is used during $t \in [0.6, 1.5]$ s to make the effect of the high-frequency amplification in the performance measure of comparable magnitude as the low-frequency effect (due to the acceleration part) during $t \in [0.38, 0.6]$ s. This way, both effects will be reflected in the performance measure in (13). Of course, depending on the application at hand, other performance measures may be defined, resulting in a different quantification of performance. As we will see in Section V, the performance measure in (13) and (14) will indeed capture the tradeoff between low-frequency disturbance suppression and sensitivity to high-frequency disturbances. The extremum-seeking approach from Section III will be used to optimally balance this tradeoff in a more desirable manner by adaptively tuning a variable gain controller.

V. Experimental Extremum-Seeking Results

In this section, the extremum-seeking control approach (Fig. 3), is used to optimally design the dead-zone length δ of the variable-gain controller (Fig. 1). Assumptions A1 and A2 from Section III-B have been satisfied in Sections IV-B and IV-C, respectively. Moreover, as we will see from the experimental results in this section, condition A3 is also satisfied for the range of values δ that we are interested in. Regarding condition A4, the following remark is in place.

Remark 4: As stated in Assumption A4, in [7], it is actually assumed that the dynamics $f(x, \delta, w)$ in (4) (Fig. 3) is twice continuously differentiable with respect to δ. However, the use of the dead-zone nonlinearity $\varphi(e, \delta)$, as shown in Fig. 2, violates this smoothness assumption. Alternatively, it would be possible to define a sufficiently smooth variant of $\varphi(e, \delta)$ which can arbitrarily closely approximate the dead-zone nonlinearity. However, for reasons related to the ease of implementation of a nonsmooth piecewise linear dead-zone characteristic, we prefer the usage of the dead-zone nonlinearity, as shown in Fig. 2. Although Assumption A4 is strictly not satisfied, it does still lead to the successful convergence of the extremum-seeking scheme, which will be illustrated by the experimental results in this section.

TABLE I
Default Extremum-Seeking Parameter Set

Parameter	c [1/s]	a [μm]	$\omega = 2\pi/T$ [rad/s]
Value	0.3	0.05	$2\pi/10$

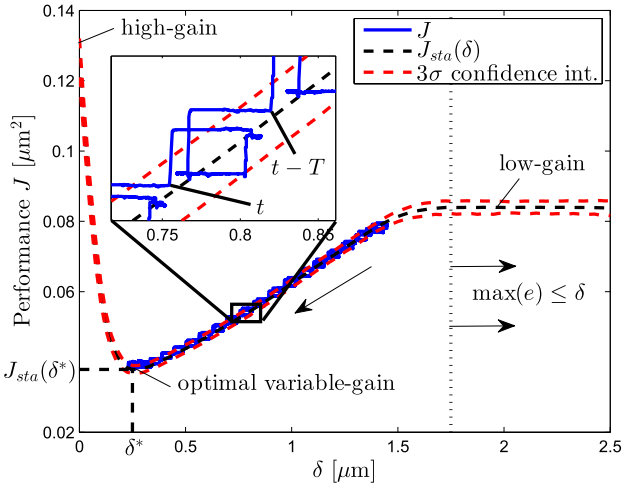

Fig. 9. Extremum-seeking result showing convergence to the dead-zone length δ^*, verified by the measured steady-state performance curve $J_{\text{sta}}(\delta)$ with 3σ confidence interval.

The set of extremum-seeking parameters as in Table I is used, unless stated otherwise. To give a motivation for the selected parameters and to give some guidelines for selecting parameters in other applications, consider the following essential aspects.

1) *The dither amplitude a* directly relates to the size of the set to which the extremum-seeking controller will converge (Figs. 9 and 10). In the variable-gain control application considered, the dead-zone length δ is known to be positive to make sense (Fig. 2). Moreover, based on the default linear low-gain and high-gain controller response (as we will see later in Fig. 11), we know that the maximum error $\max(|e|) \leq 1.75$ μm such that for $\delta \geq 1.75$ μm, the linear low-gain controller will be effective. The interesting range for δ is thus given by $0 \leq \delta \leq 1.75$ μm. A dither amplitude of 0.05 μm ($\approx 3\%$ of the interested range of 1.75 μm) is therefore selected as an initial choice for the dither amplitude a.
2) *The dither frequency ω* should be selected sufficiently low to guarantee that the performance $J(t, \delta)$ is close to

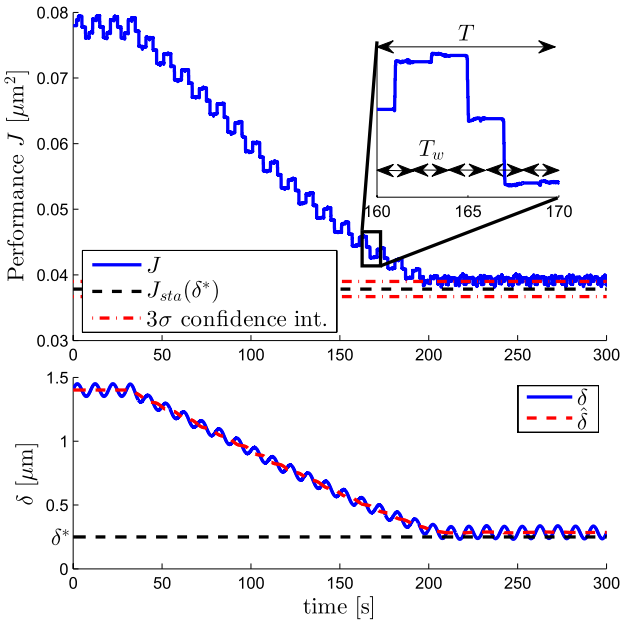

Fig. 10. Convergence of the dead-zone length δ and performance $J(t, \delta)$.

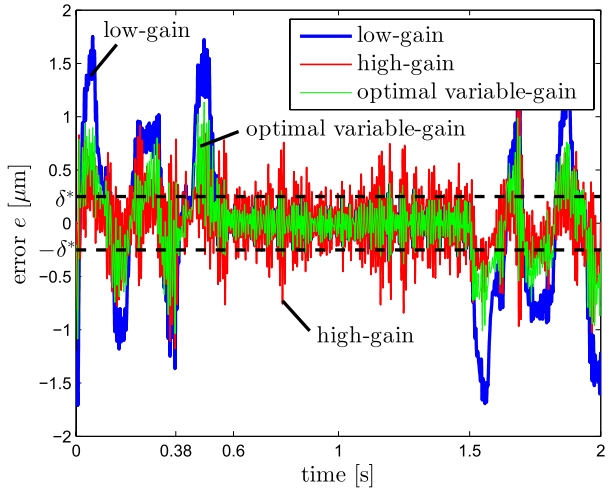

Fig. 11. Measured tracking error for the low-gain, high-gain, and optimized variable-gain controller.

the steady-state performance map $J_{\text{sta}}(\delta)$ (Fig. 4). Note that to guarantee this time-scale separation, first of all, the stabilized plant $\dot{x} = f(x, \delta, w(t))$ (Fig. 3) should be sufficiently fast compared with the dither signal, which is standard in the extremum-seeking literature. Second of all, we should choose T sufficiently larger than T_w, such that δ is perceived as constant over one period T_w (see the discussion on time-scale separation in Section III-A). Therefore, we choose $T = 2\pi/\omega = 10$ s, a factor 5 larger than the period $T_w = 2$ s of the input $w(t)$.

3) *The adaptation gain* c should be chosen small enough, again to guarantee the time-scale separation (Fig. 4). Over one period of the dither T, the nominal value for $\hat{\delta}$ (Fig. 3) should not change too much compared with the dither to obtain an accurate gradient estimate. Since $\dot{\hat{\delta}} = -c\widetilde{\partial J}/\partial\delta$, the choice for c relates to the gradient of the performance map, which is in general unknown. For an initial experiment, it is therefore sensible to start with a very small c (such that the $\hat{\delta}$ changes very slowly) and increase it gradually to achieve a desirable convergence rate, which resulted in $c = 0.3$ s^{-1}, for the settings of a and ω in Table I.

Consider the experimental extremum-seeking results in Fig. 9. To validate the results of the extremum-seeking controller, the steady-state performance curve $J_{\text{sta}}(\delta)$, which is in general unknown, has been experimentally identified. The static performance curve J_{sta} was obtained by measuring the steady-state response for 100 linearly distributed δs in the range $[0, 2.5]$ μm. Since there is some variation between subsequent experiments, due to slightly changing operating conditions, the curve has been measured 10 different times, such that we are able to plot the averaged curve and the 3σ confidence interval in Fig. 9. Note that this (slow) variation in performance can be perfectly compensated for by the extremum-seeking controller (if it is on a slower time-scale than the adaptation mechanism of the extremum seeker, which is the case here), since it will continuously adapt to find the minimum of the performance curve.

In Fig. 10, the performance J and dead-zone length δ are shown in time. As an initial dead-zone length, we chose $\delta = 1.4$ μm. Initially, we set $c = 0$ and wait $\sim$30 s (3 dither periods of $T = 10$ s) before enabling the adaptation (Fig. 10). This guarantees that the plant has enough time to converge to its steady-state values and moreover, due to the moving average filter with $T = 2\pi/\omega = 2$ s of history and the performance measure $J(t, \delta)$ with $T_w = 10$ s of history, it takes at least $T + T_w = 12$ s to build up information on the steady-state performance. Clearly, Figs. 9 and 10 show that the extremum-seeking controller converges to a region around the performance-optimal dead-zone length of $\delta^* \approx 0.25$ μm, with corresponding optimal performance $J_{\text{sta}}(\delta) = 0.038$ μm^2 (where δ^* and $J_{\text{sta}}(\delta^*)$ correspond to the minimum of the measured steady-state performance curve in Fig. 9; the same optimal values are plotted in Fig. 10). It takes approximately 200 s for the extremum-seeking controller to converge to this optimum. The oscillations in the performance measure $J(t, \delta)$ relate to the period $T = 10$ s of the dither signal. Note that the period of the external inputs $T_w = 2$ s is visible from the zoom-plot in the upper plot in Fig. 10. The constant parts in the zoom-plot are a result of the 0-segments in the selection function $s(t)$ in Fig. 8. After the 0-segments, new relevant error-data is used in the performance measure (5), resulting in the change of the performance $J(t, \delta)$.

In terms of the performance measure $J(t, \delta)$, the optimized variable-gain controller outperforms the linear low-gain ($\delta \geq 1.75$ μm) and high-gain ($\delta = 0$) controllers by 55% and 70%, respectively, as we can conclude from Fig. 9. However, the true performance improvement should of course also be reflected in the measured tracking error $e(t)$, which is shown in Fig. 11. The goal of the variable-gain controller was to improve the low-frequency response (due to the acceleration phases with nonperfect feed-forward compensation) while not deteriorating the high-frequency error response during the constant position part of the set point $r(t)$ (Fig. 8). Indeed,

the variable gain controller achieves this goal, as can be concluded from Fig. 11 that the noise response of the optimal variable gain controller during $t \in [0.6, 1.5]$ s is similar to the low-gain controller, because the error $e(t)$ stays within the optimized dead-zone length δ^*. In addition, it improves the low-frequency error response during the acceleration part for $t \in [0.38, 0.6]$ s because additional gain is applied for the large low-frequency errors outside the dead-zone band. Note that the performance measure as defined in (13) and (14) was therefore a good performance measure that captures the tradeoff between low-frequency disturbance suppression and sensitivity to high-frequency disturbances.

Remark 5: The experimental implementation of the extremum-seeking loop (Fig. 3) is performed on a digital computational platform. In the experiments conducted here, the variable-gain control loop was implemented at a sampling frequency of 5 kHz, and the extremum-seeking controller and computation of the performance $J(t, \delta)$ was implemented at a reduced sampling frequency of 50 Hz. We have chosen for such a dual-rate implementation for two reasons. First, due to limited computational recourses or limited memory, it may in practice be impossible to carry out all the extremum-seeking computations at the same sampling rate as the variable-gain control loop. Second, due to the time-scale separation between the motion control dynamics and the extremum-seeking loop (including the computation of the performance measure), it is both reasonable and justified to run the latter at a much lower sampling rate than the motion controller.

A. Supporting Experiments

The default parameter selection as in Table I will be changed here to investigate the effect of the tuning of the parameters of the extremum seeking controller on the performance of the extremum-seeking loop for periodic steady states. In particular, we investigate the role of the time-scale separation between the input period T_w and the dither period T, which is specific for the extremum-seeking in terms of periodic steady-states. Based on these experimental results, we will formulate some tuning guidelines for the selection of the dither period T.

1) Choice of Dither Amplitude a and Adaptation Gain c: Increasing the adaptation gain c will speed up the convergence of the extremum-seeking controller (Fig. 12). Of course, it cannot be chosen too large because then the time-scale separation brakes down, i.e., the performance $J(t, \delta)$ will not remain close to the steady-state performance map $J_{\text{sta}}(\delta)$ (Fig. 4). Increasing the dither amplitude a allows the adaptation gain c to be chosen larger, but this also results in a larger neighborhood around the optimum δ^* to which the extremum-seeking controller converges (Fig. 12). This tradeoff between speed of adaptation and neighborhood of convergence is well known, also in the extremum-seeking setting for equilibria [17], [25], [26].

2) Choice of Dither Frequency $\omega = 2\pi/T$: The dither frequency $\omega = 2\pi/T$ should be chosen sufficiently small, compared with the time-scale of the plant and the external T_w-periodic inputs (see the discussion on time-scales in Section III-A). In the variable-gain control application,

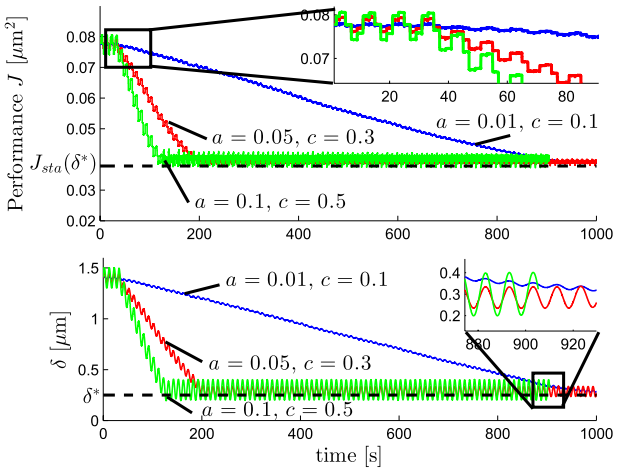

Fig. 12. Influence of dither amplitude a and adaptation gain c on extremum-seeking experiments.

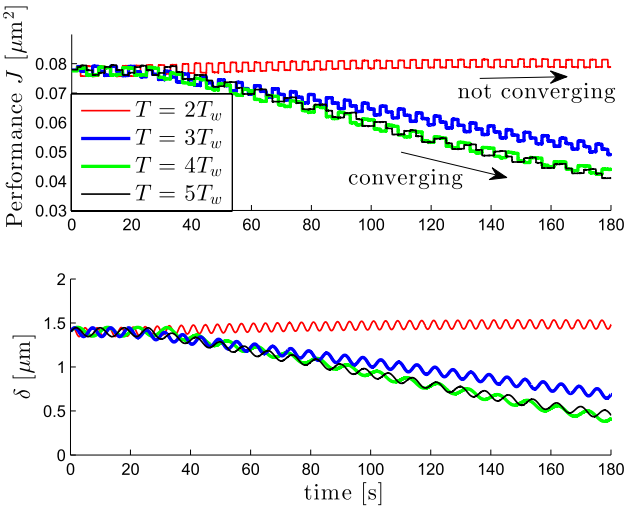

Fig. 13. Influence of dither frequency $\omega = 2\pi/T$ on extremum-seeking experiments.

the period T_w of the input is typically larger than the time-scale of the plant, since the references that are to be tracked have frequency content that lies well below the bandwidth of the system. Hence, the dither period T should be chosen sufficiently larger than the period T_w of the external reference. The results in Fig. 13 show the influence of the choice of dither period T for a fixed value of $T_w = 2$ s. The dither periods $T \in \{2T_w, 3T_w, 4T_w, 5T_w\}$ are used in Fig. 13. Clearly, if T is chosen too small, the extremum-seeking controller does not converge anymore to the performance optimal δ^*. For the choice $T = 3T_w$, the extremum-seeking controller still converges (Fig. 13), but the gradient $\partial J_{\text{sta}}/\partial\delta$ is underestimated, resulting in a slightly slower convergence than for $T = 4T_w$ and $T = 5T_w$. Note that if T is chosen sufficiently larger than T_w, for each T_w s, the δ is perceived as constant such that $J(t, \delta)$ is close to the steady-state performance and, hence, giving an accurate estimate of the gradient of the steady-state performance map $J(\delta)$. We therefore recommend to choose at least $T \geq 4T_w$. A too large value for the dither period T

(or, equivalently, too small value for the dither frequency ω) should, however, be avoided since this may require a smaller value for the optimizer gain c, which slows down the convergence rate.

VI. Conclusion

In this paper, we have experimentally demonstrated an extremum-seeking control strategy for time-varying periodic steady-states for the adaptive design of variable-gain controllers. A performance-relevant parameter, the dead-zone length of a nonlinear variable-gain controller, has been tuned successfully using the extremum-seeking control strategy, without using explicit knowledge on the disturbances acting on the system. The optimized variable gain controller outperforms the linear motion controllers by balancing the tradeoff between low-frequency disturbance rejection and sensitivity to high-frequency disturbances in a more desirable manner. This paper evidences the importance and practical applicability of the extremum-seeking control scheme for nonlinear systems with time-varying periodic steady-state outputs.

In addition to the adaptive tuning of the variable-gain feedback controller, we foresee an interesting combination with the adaptive tuning of feed forward to further enhance the performance of variable-gain controlled motion systems.

References

[1] K. H. Ang, G. Chong, and Y. Li, "PID control system analysis, design, and technology," *IEEE Trans. Control Syst. Technol.*, vol. 13, no. 4, pp. 559–576, Jul. 2005.

[2] K. B. Ariyur and M. Krstić, *Real-Time Optimization by Extremum-Seeking Control*. Hoboken, NJ, USA: Wiley, 2003.

[3] B. S. R. Armstrong, J. A. Guitierrez, B. A. Wade, and R. Joseph, "Stability of phase-based gain modulation with designer-chosen switch functions," *Int. J. Robot. Res.*, vol. 25, no. 8, pp. 781–796, 2006.

[4] B. P. Demidovich, "Dissipativity of a nonlinear system of differential equations," *Ser. Mat. Mekh.*, Part I-6:19–27, 1961.

[5] J. Freudenberg, R. Middleton, and A. Stefanopoulou, "A survey of inherent design limitations," in *Proc. Amer. Control Conf.*, Chicago, IL, USA, 2000, pp. 2987–3001.

[6] M. Guay, D. Dochain, M. Perrier, and N. Hudon, "Flatness-based extremum-seeking control over periodic orbits," *IEEE Trans. Autom. Control*, vol. 52, no. 10, pp. 2005–2012, Oct. 2007.

[7] M. Haring, N. van de Wouw, and D. Nešić, "Extremum-seeking control for nonlinear systems with periodic steady-state outputs," *Automatica*, vol. 49, no. 6, pp. 1883–1891, 2013.

[8] M. Heertjes, T. Tepe, and H. Nijmeijer, "Multi-variable iterative tuning of a variable gain controller with application to a scanning stage system," in *Proc. Amer. Control Conf. (ACC)*, San Francisco, CA, USA, 2011, pp. 816–820.

[9] M. Heertjes, B. Hunnekens, N. van de Wouw, and H. Nijmeijer, "Learning in the synthesis of data-driven variable-gain controllers," in *Proc. Amer. Control Conf.*, Washington, DC, USA, 2013, pp. 6685–6690.

[10] M. Heertjes and G. Leenknegt, "Switching control in blu-ray disk drives," *Mechatronics*, vol. 20, no. 4, pp. 453–463, 2010.

[11] M. F. Heertjes, X. G. P. Schuurbiers, and H. Nijmeijer, "Performance-improved design of N-PID controlled motion systems with applications to wafer stages," *IEEE Trans. Ind. Electron.*, vol. 56, no. 5, pp. 1347–1355, May 2009.

[12] K. Höffner, N. Hudon, and M. Guay, "On-line feedback control for optimal periodic control problems," *Can. J. Chem. Eng.*, vol. 85, no. 4, pp. 479–489, 2007.

[13] B. G. B. Hunnekens, M. A. M. Haring, N. van de Wouw, and H. Nijmeijer, "Steady-state performance optimization for variable-gain motion control using extremum seeking," in *Proc. IEEE Conf. Decision Control*, Maui, HI, USA, 2012, pp. 3796–3801.

[14] H. K. Khalil, *Nonlinear Systems*. Upper Saddle River, NJ, USA: Prentice-Hall, 2002.

[15] S. Z. Khong, D. Nešić, Y. Tan, and C. Manzie, "Unified frameworks for sampled-data extremum seeking control: Global optimisation and multi-unit systems," *Automatica*, vol. 49, no. 9, pp. 2720–2733, 2013.

[16] M. Krstić and H.-H. Wang, "Stability of extremum seeking feedback for general nonlinear dynamic systems," *Automatica*, vol. 36, no. 4, pp. 595–601, 2000.

[17] D. Nešić, "Extremum seeking control: Convergence analysis," *Eur. J. Control*, vol. 15, nos. 3–4, pp. 331–347, 2009.

[18] D. Nešić, Y. Tan, W. H. Moase, and C. Manzie, "A unifying approach to extremum seeking: Adaptive schemes based on estimation of derivatives," in *Proc. 49th IEEE Conf. Decision Control (CDC)*, Atlanta, GA, USA, Dec. 2010, pp. 4625–4630.

[19] A. Pavlov, B. G. B. Hunnekens, N. van de Wouw, and H. Nijmeijer, "Steady-state performance optimization for nonlinear control systems of Lur'e type," *Automatica*, vol. 49, no. 7, pp. 2087–2097, 2013.

[20] A. Pavlov, N. van de Wouw, and H. Nijmeijer, *Uniform Output Regulation of Nonlinear Systems: A Convergent Dynamics Approach*. Boston, MA, USA: Birkhäuser, 2005.

[21] A. Pavlov, N. van de Wouw, and H. Nijmeijer, "Frequency response functions for nonlinear convergent systems," *IEEE Trans. Autom. Control*, vol. 52, no. 6, pp. 1159–1165, Jun. 2007.

[22] M. M. Seron, J. H. Braslavsky, and G. C. Goodwin, *Fundamental Limitations in Filtering and Control*. Berlin, Germany: Springer-Verlag, 1997.

[23] M. Steinbuch and M. L. Norg, "Advanced motion control: An industrial perspective," *Eur. J. Control*, vol. 4, no. 4, pp. 278–293, 1998.

[24] Y. Tan, W. H. Moase, C. Manzie, D. Nešić, and I. Mareels, "Extremum seeking from 1922 to 2010," in *Proc. 29th Chin. Control Conf.*, Beijing, China, Jul. 2010, pp. 14–26.

[25] Y. Tan, D. Nešić, and I. Mareels, "On non-local stability properties of extremum seeking control," *Automatica*, vol. 42, no. 6, pp. 889–903, 2006.

[26] Y. Tan, D. Nešić, and I. Mareels, "On the choice of dither in extremum seeking systems: A case study," *Automatica*, vol. 44, no. 5, pp. 1446–1450, 2008.

[27] A. R. Teel and D. Popovic, "Solving smooth and nonsmooth multivariable extremum seeking problems by the methods of nonlinear programming," in *Proc. Amer. Control Conf.*, vol. 3. Arlington, VA, USA, 2001, pp. 2394–2399.

[28] T. Tuma, A. Pantazi, J. Lygeros, and A. Sebastian, "Nanopositioning with impulsive state multiplication: A hybrid control approach," *IEEE Trans. Control Syst. Technol.*, vol. 21, no. 4, pp. 1352–1364, Jul. 2013.

[29] N. van de Wouw, H. A. Pastink, M. F. Heertjes, A. Pavlov, and H. Nijmeijer, "Performance of convergence-based variable-gain control of optical storage drives," *Automatica*, vol. 44, no. 1, pp. 15–27, 2008.

[30] V. Yakubovich, "The matrix inequality method in the theory of the stability of nonlinear control systems—I. The absolute stability of forced vibrations," *Autom. Remote Control*, vol. 25, pp. 905–917, 1964.

[31] J. Zheng, G. Guo, and Y. Wang, "Nonlinear PID control of linear plants for improved disturbance rejection," in *Proc. 16th IFAC World Congr. (IFAC)*, Prague, Czech Republic, 2005, p. 1256.

Bram Hunnekens was born in 1987. He received the M.Sc. (*cum laude*) degree in dynamics and control from the Eindhoven University of Technology, Eindhoven, The Netherlands, in 2011, where he is currently pursuing the Ph.D. degree with the Department of Mechanical Engineering.

His current research interests include nonlinear control of linear motion systems and performance-optimal nonlinear controller synthesis.

Antonio Di Dino was born in Monselice, Italy, in 1983. He received the M.Sc. and Ph.D. degrees in mechatronics engineering from the University of Trento, Trento, Italy, in 2010 and 2014, respectively. His Ph.D. thesis was entitled Design and Development of a Distributed System for Monitoring of Machine Tool Behavior.

He is currently a Mechatronics Design Engineer with the Department of Research and Development, PAMA s.p.a., Rovereto, Italy.

Nathan van de Wouw (M'08) was born in 1970. He received the M.Sc. (Hons.) degree and the Ph.D. degree in mechanical engineering from the Eindhoven University of Technology, Eindhoven, The Netherlands, in 1994 and 1999, respectively.

He is with the Department of Mechanical Engineering, Eindhoven University of Technology, from 1999 to 2014, as an Assistant/Associate Professor. He was with Philips Applied Technologies, Eindhoven, in 2000, and the Netherlands Organization for Applied Scientific Research, Delft, The Netherlands, in 2001. He held Visiting Professor positions with the University of California at Santa Barbara, Santa Barbara, CA, USA., from 2006 to 2007, the University of Melbourne, Melbourne, VIC, Australia, from 2009 to 2010, and the University of Minnesota, from 2012 to 2013. He currently holds an Adjunct Full Professor position with the University of Minnesota, Minneapolis, MN, USA. He has authored a large number of journal and conference papers and the books entitled *Uniform Output Regulation of Nonlinear Systems: A Convergent Dynamics Approach* (Birkhauser, 2005), with A.V. Pavlov and H. Nijmeijer, and *Stability and Convergence of Mechanical Systems with Unilateral Constraints* (Springer-Verlag, 2008), with R.I. Leine. His current research interests include the analysis and control of nonlinear/nonsmooth systems and networked control systems.

Prof. Wouw is currently an Associate Editor of the *Automatica* and the IEEE TRANSACTIONS ON CONTROL SYSTEMS TECHNOLOGY journals.

Niels van Dijk received the M.Sc. and Ph.D. degrees in mechanical engineering from the Eindhoven University of Technology, Eindhoven, The Netherlands, in 2006 and 2011, respectively.

He has been with the Mechatronics Technologies Group, Philips Innovation Services, Eindhoven, since 2011. His current research interests include the analysis and control of mechatronic systems for the semiconductor, and medical industry.

Henk Nijmeijer (F'99) was born in 1955. He received the M.Sc. degree and the Ph.D. degree in mathematics from the University of Groningen, Groningen, The Netherlands, in 1979 and 1983, respectively.

He was with the Department of Applied Mathematics, University of Twente, Enschede, The Netherlands, from 1983 to 2000. Since 1997, he has been with the Department of Mechanical Engineering, Eindhoven University of Technology, Eindhoven, The Netherlands. Since 2000, he has been a Full Professor with the Eindhoven University of Technology, where he chairs the Dynamics and Control Section. He has authored a large number of journal and conference papers, and several books, including the *Nonlinear Dynamical Control Systems* (Springer, 1990), with A. J. van der Schaft, *Synchronization of Mechanical Systems* (World Scientific, 2003), with A. Rodriguez, *Dynamics and Bifurcations of Non-Smooth Mechanical Systems* (Springer-Verlag, 2004), with R. I. Leine, and *Uniform Output Regulation of Nonlinear Systems* (Birkhauser, 2005), with A. Pavlov and N. van de Wouw.

Prof. Nijmeijer is currently an Honorary Knight of the Golden Feedback Loop at the Norwegian University of Science and Technology, Trondheim, Norway. He is a Board Member of the Dutch Institute on Systems and Control, a Council Member of the International Federation of Accountants, and is/has been the Organizer and/or IPC Chair of numerous international conferences and workshops. He was a recipient of the IEE Heaviside Premium Award in 1990. He is an Editor of the *Communications on Nonlinear Systems and Numerical Simulation*, a Corresponding Editor of the *SIAM Journal on Control and Optimization*, and a Board Member of the *International Journal of Control*, *Automatica*, the *Journal of Dynamical Control Systems*, the *International Journal of Bifurcation and Chaos*, *International Journal of Robust and Nonlinear Control*, *Journal of Nonlinear Dynamics*, and the *Journal of Applied Mathematics and Computer Science*.